Reactivity of 3-Methylbenzenediazonium Ions with Gallic Acid. Kinetics and Mechanism of the Reaction

by **Sonia Losada-Barreiro** and **Carlos Bravo-Díaz***

Universidad de Vigo, Facultad de Ciencias, Dpto. Química Física, ES-36200 Vigo
(fax: +986-812556; e-mail: cbravo@uvigo.es)

We investigated the kinetics and mechanism of the reaction between the 3-methylbenzenediazonium ions (3MBD), and gallic acids (= 3,4,5-trihydroxybenzoic acid; GA) in aqueous buffer solution under acidic conditions by employing spectrometric, electrochemical, and chromatographic techniques and computational methods. To discern which of the three OH groups of GA is the first one undergoing deprotonation, the geometries of the resulting dianions were optimized by using B3LYP hybrid density-functional theory (DFT) and a 6-31G(++d,p) basis set, and the results suggest that the OH group at the 4-position is the first one which is deprotonated. The variation of the observed rate constant, k_{obs}, with the acidity at a given [GA] follows an upward curve suggesting that the reaction takes place with the dianionic form of gallic acid, GA^{2-}, and rate enhancements of *ca.* 23000 fold are obtained on going from pH 3.5 up to pH 7.5. At relatively high acidities, the variation of k_{obs} with [GA] is linear with an intercept very close to the value for the thermal decomposition of 3MBD; however, a decrease in the acidity leads to saturation-kinetics profiles with nonzero, pH-dependent intercepts. The saturation-kinetics patterns found suggest the formation of an intermediate in a rapid pre-equilibrium step, but the nonzero, pH-dependent intercepts cause the double reciprocal plots of $1/k_{obs}$ *vs.* 1/[GA] to curve. This prompts us to propose an alternative reaction mechanism comprising consecutive equilibrium processes involving the bimolecular, reversible formation of a highly unstable (*Z*)-diazo ether which undergoes isomerization to the (*E*)-isomer through a unimolecular step. The results obtained indicate the complexity of reactions of arenediazonium ions with nucleophilic arenes containing three or more OH groups.

Introduction. – Arenediazonium ions, ArN_2^+, have been the subject of mechanistic investigations for a long time because of their extensive use in chemistry [1–4]. Summarizing their mechanisms, two commonly encountered kinds of reactions are involved; those involving elimination of nitrogen (dediazoniation reactions; *Scheme 1*,*a*) and those featuring retention of nitrogen (*Scheme 1*,*b*) [1][2][4]. Typical examples of the latter are the well-known reactions of arenediazonium ions with phenols and naphthalenols (*Scheme 1*,*b*) which are usually referred as C-coupling reactions [1–9] and constitute a typical example of an electrophilic aromatic-substitution (EAS) reaction.

The general EAS mechanism (*Scheme 1*,*b*) involves a first fast equilibrium between the electron-rich aromatic substrate and the electron-deficient reagent. The formation of a donor–acceptor complex [3][4][10][11] (not shown) is followed by another equilibrium (or an irreversible step) producing the σ-complex (the *Wheland* intermediate, W). The formation of a donor–acceptor complex is corroborated by numerous spectroscopic transient observations or by isolation [12–14]. Generally, the rate-limiting step of the overall reaction is considered to be the formation of the σ-

Scheme 1. a) *Basic Representation of the Thermal Decomposition of* ArN_2^+ ($D_N + A_N$ mechanism), b) *that of the Electrophilic-Aromatic-Substitution Mechanism Leading to the Formation of a Stable Azo Dye* (B = any base), *and* c) *that of the Reaction with* RO^- (or ROH followed by proton loss) *Leading to the Formation of a Diazo Ether*

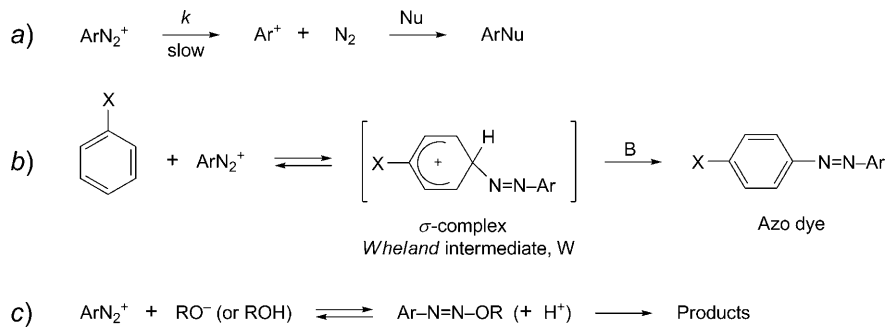

adduct W (in which case this step must be irreversible), and the substitution products P are obtained by proton loss in a fast, irreversible step [10][11].

Because arenediazonium ions are relatively weak electrophiles [1][2][4], C-coupling reactions take place with substances containing OH or NH_2 groups, which increase the C-nucleophilicity of the coupling component. The reactions are strongly affected by the pH; aromatic amines react through the free base, while the reactive species in the reaction with phenols or naphthalenols are the phenoxide or naphthalenolate ions, which react as much as 10^{10} times faster than the nonionized forms [1][3][15]. The presence of two ionizable groups (*e.g.*, two OH groups) at the nucleophilic arene parent structure increases the reactivity of the substrate, but their effect is not additive and depends strongly on their relative positions at the benzene ring [1][2][4]. For instance, resorcinol (= benzene-1,3-diol) has two nucleophilic centers able to couple, with the dianion coupling more than 10^4 times faster than the monoanion coupling [4][16]. In contrast, catechol (= benzene-1,2-diol) and hydroquinone (= benzene-1,4-diol) are oxidized by ArN_2^+ ions.

When the *o*- and *p*-positions of the OH groups are blocked or not sufficiently activated, O-coupling reactions leading to the formation of diazo ethers may take place (*Scheme 1,c*). For instance, the reaction of toluenediazonium ions with ascorbic acid [17][18] and methyl gallate [19] proceed through the formation and decomposition of diazo ether intermediates. Diazo ethers are, however, rather unstable and can only be isolated under favorable conditions [20] although, in some instances, their formation and decomposition can be detected experimentally [17–19][21].

We recently investigated the reaction of the 3-methylbenzenediazonium ion (3MBD) with methyl gallate (= methyl 3,4,5-trihydroxybenzoate; MG), concluding that the reaction takes place through the rapid formation of an unstable O-coupling adduct in a pre-equilibrium step followed by a unimolecular, rate-determining decomposition [19]. In the course of these reactions, biphasic kinetics associated with the formation and subsequent decomposition of the transient diazo ether were found experimentally. We have also studied the micellar effects on the reaction of 3MBD with gallic acid (GA) and octyl gallate [22], and surprisingly, the kinetic profiles were

not biphasic: the absorbance at λ 416 nm due to product formation remained practically constant after leveling off. Also, the reaction between 3MBD and GA in aqueous acid solution did not show biphasic kinetic profiles (see *Exper. Part*).

These unexpected observations may need extra attention because the effects of substituents in the pyrogallol (= benzene-1,2,3-triol) moiety are currently unknown, and thus we expanded our previous investigations and report here the results of a detailed kinetic study on the reaction between 3MBD and GA in aqueous acid solution. The aim of this study is two-fold. First, to expand our current knowledge on the reactions of arenediazonium ions with polyhydroxylated antioxidants as they have been very much less investigated than those with the mono- and dihydroxylated phenol derivatives [1][4]. Previous dediazoniation work with antioxidants such as ascorbic acid or methyl gallate, which do not possess structures able to build up very high electron densities at one or more C-atoms, showed that the reactions do not proceed through the C-coupling pathway but *via* the formation of transient diazo ethers [17][18][23][24].

Secondly, knowledge of the reaction mechanism of polar organic molecules such as antioxidants may be valuable in determining their distribution in emulsified systems [25][26]. Gallic acid is a basic structural unit of hydrolyzable tannins widely distributed in the plant kingdom especially in tanniferous plants in conjunction with other important polyphenolic compounds widely used as antioxidants [27–29]. Estimating its distribution (and that of its derivatives) in food emulsions is important because their efficiency in inhibiting lipid peroxidation depends, among other aspects, on their distribution within the different regions of the system [26][30][31].

For these purposes, we employed a combination of computational methods and spectrometric, electrochemical, and chromatographic measurements. As we will show, the kinetic behavior found is more complex than that observed for the reaction with MG in spite of the reactions sharing some common kinetic features. The experimental results appear to be consistent with consecutive reversible steps involving a fast, bimolecular step, in which 3MBD associates with GA^{2-} to form a (*Z*)-diazo ether complex which is subsequently isomerized to the ionized form of the much more stable (*E*)-diazo ether in a slow unimolecular step.

Results. – 1. *Ionization Position of GA: Density Functional Theory (DFT) Studies.* Gallic acid (**1A** in *Scheme 2*) has four ionizable OH groups and, therefore, can exist in five different molecular forms depending on the working pH. While the pK_{a1} and pK_{a2} values can be easily determined from potentiometric or spectrophotometric titrations, the pK_{a3} and pK_{a4} values are not known accurately because of the instability of gallates to oxidation in alkaline solution [32][33]. The first acidity constant (pK_{a1} *ca.* 4.2) is associated with ionization of the carboxylic acid (→ **1B**) [34][35]. The second one, pK_{a2} *ca.* 8.6 [34], is likely to be associated with the OH group in the 4-position (→ **1C** in *Scheme 2*) because this allows delocation of the negative charge, and the presence of two *ortho*-positioned OH groups stabilizes the negative charge by intramolecular H-bonds (see **1E**). This assumption is supported by computational evidence employing B3LYP DFT with a 6-31G(++d,p) basis set. A complete geometry optimization was carried out for the isomeric dianions and their energies compared with that of the monoanion. The results show that **1E** has an energy *ca.* 36 kJ/mol lower than that of **1F**

Scheme 2. *Ionization of Gallic Acid and Some of the Possible Resonance Forms* (**1C** and **1D**) *Showing the Intramolecular H-Bonds.* The optimized structure **1E**, showing the ionization in the 4-position, lies lower in energy than structure **1F**.

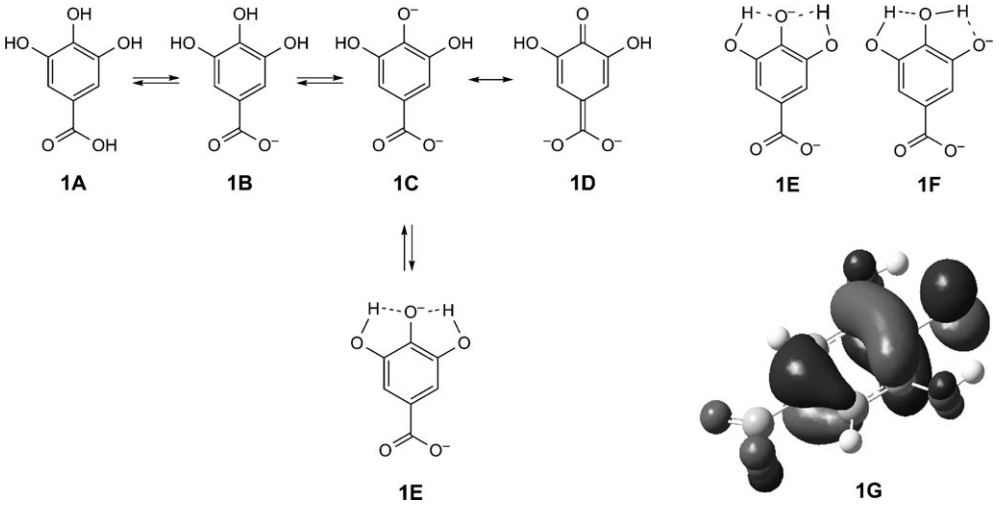

and that the highest electron density (HOMO orbital) is located on the 4-O-atom (see **1G**).

The geometry of structure **1G** is the same as that of **1E** but shows the HOMO orbitals as determined by DFT theory (B3LYP, 6-31G(+ + d,p) basis set), illustrating that the highest electron density is located at the O-atom at C(4) of GA, little electron density is at the O-atoms at C(3) and C(5), and negligible electron density at the C(2) and C(6) atoms. The results suggest that an electrophilic attack is likely to take place on the O-atom at C(4) (O-coupling) rather than on the O-atoms at C(3) and C(5) or on the C(2) and C(6) atoms (C-coupling).

2. *Effects of Acidity on* k_{obs}. As noted before, GA behaves as a weak acid, and there exists the possibility of reaction between ArN_2^+ and the carboxylate ions. Literature reports [1][2][4] indicate that the reaction between ArN_2^+ and acetate ions proceed, as most of the O-coupling reactions, through an equilibrium step; however, the equilibrium lies very much on the side of the starting ions ($K = 10^{-5}$ M^{-1}). Thus, it appears that a hypothetical reaction with the O-atom of the carboxylate group should be negligible. However, we tested the possibility by analyzing the dependence of k_{obs} with the acidity of the medium. Clean first-order behavior was obtained in all runs for at least three half-lives. *Fig. 1* shows the dependence of k_{obs} with pH, its variation following an upward curve with k_{obs} increasing about 23000 times on going from pH 3.5 up to pH 7.5. Higher acidities were not employed because reactions become too slow, with k_{obs} *ca.* $(4.0 \pm 0.2) \cdot 10^{-4}$ s^{-1}, a value very similar to that for the thermal decomposition of 3MBD [36], $k_{obs} = 3.5 \cdot 10^{-4}$ s^{-1}. At lower acidities, the reactions become too fast to be monitored and were not employed to minimize GA autooxidation, which may be appreciable in alkaline solution [32][33]. The variation

of $\log(k_{obs})$ with pH is linear (*Fig. 1*), with a slope of 1.03 ± 0.04, indicating an inverse dependence of k_{obs} with $[H^+]$.

The inset in *Fig. 1* is an amplification of the pH 3–5 region, showing that no significant changes in k_{obs} are detected upon ionization of the carboxylic group of GA (pK_a *ca.* 4.3) suggesting, therefore, that the reaction is taking place through the dianionic form of GA^{2-} of GA. Similar results were found when employing different [GA].

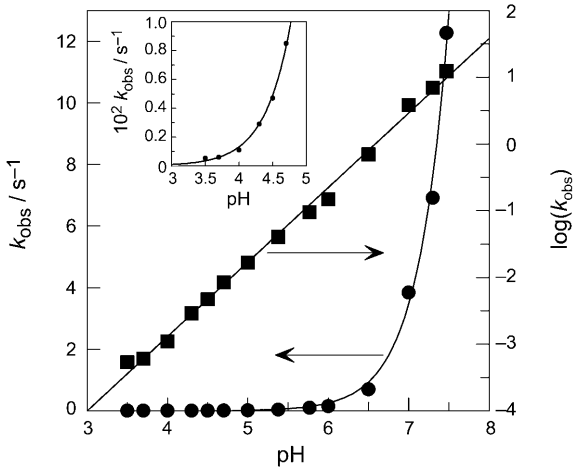

Fig. 1. *Variation of* k_{obs} *with pH and representation of log(*k_{obs}*) with pH at a given [GA].* The inset is an amplification of the pH 3–5 range. Very similar results were obtained at different [GA], with average slopes of 1.03 ± 0.04, indicative of an inverse dependence of k_{obs} with $[H^+]$. $[3MBD]_{initial} = 3.1 \cdot 10^{-4}$ M, *T* 30°.

Auxiliary experiments were carried out by intentionally changing the nature of the buffer and its concentrations (*Table 1*). Addition of different amounts of a base ([pyridine] = 0.01–0.2M) revealed no significant changes in k_{obs}, indicating that proton loss is not involved in the rate-limiting step and that the reaction is not general-base-catalyzed.

Table 1. *Effects of Buffer and Base* (pyridine) *Concentrations on* k_{obs} *for the Reaction between 3MBD and GA.* $[3MBD]_{initial} = 3.1 \cdot 10^{-4}$ M, pH 5, *T* 30°.

[AcOH/AcO$^-$]/M	10^2 k_{obs}/s^{-1}	[py]/M	10^2 k_{obs}/s^{-1}	[py]/M	10^2 k_{obs}/s^{-1}
0.12	1.80 ± 0.03	0.000	1.70 ± 0.01	0.133	1.53 ± 0.02
0.24	1.68 ± 0.02	0.033	1.57 ± 0.02	0.167	1.51 ± 0.02
0.4	1.48 ± 0.01	0.066	1.53 ± 0.03	0.200	1.49 ± 0.02
		0.100	1.50 ± 0.02		

3. *Effects of [GA] on* k_{obs}. *Fig. 2* illustrates the variation of k_{obs} with [GA] at different acidities. At low pH (*Fig. 2,a*), relatively modest linear increases in k_{obs} upon increasing [GA] are obtained, and the intercept values, which represent the k_{obs} values in the absence of GA, are the same and equal to that for the spontaneous

decomposition of 3MBD under acidic conditions [36], $k_{obs} = 3.5 \cdot 10^{-4}$ s^{-1}. In contrast, saturation-kinetics patterns with unequal nonzero intercepts are obtained at higher pH values (*Fig. 2*,*b*).

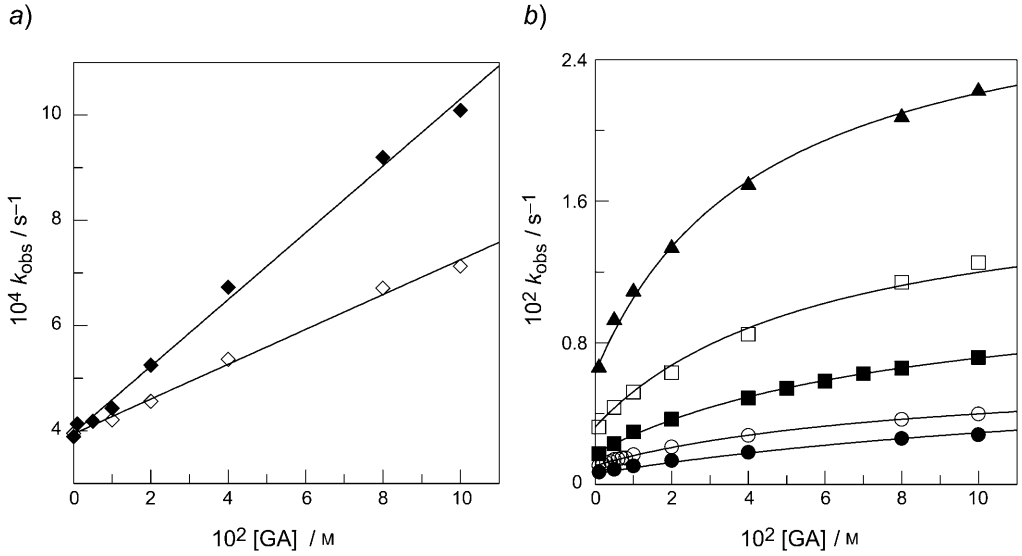

Fig. 2. *Variation of* k_{obs} *with [GA] at different acidities* (buffer control): a) *at low pH and* b) *at higher pH.* ◇ pH 3.5, ◆ pH 3.7, ● pH 4.1, ○ pH 4.3, ■ pH 4.5, □ pH 4.7, ▲ pH 5.0. [3MBD] = $3.1 \cdot 10^{-4}$ M, *T* 30°.

The finding of saturation kinetics may suggest a mechanism involving an irreversible rate-determining decomposition of a transient intermediate, which is produced in a rapid pre-equilibrium step; however, nonzero, pH-dependent intercept values are unexpected. The variation of the intercepts with acidity is illustrated in *Fig. 3*,*a*, and the corresponding values are displayed in *Table 2*.

Table 2. *Values for the Intercepts* (k_4), k_3, *and for the Ratio* k_1/k_2 (first equilibrium step in *Scheme 3*) *Determined by Fitting the Experimental Data to* Eqns. 1 *and* 2

pH	10^4 k_4/s^{-1}	10^3 k_3/s^{-1}	10^{-5} k_1/k_2
4.1	4.96 ± 0.01	4.93 ± 0.20	2.98 ± 0.14
4.3	10.58 ± 0.02	5.46 ± 3.76	2.89 ± 0.13
4.5	17.22 ± 0.05	9.92 ± 1.71	1.99 ± 0.40
4.7	32.37 ± 0.14	14.10 ± 2.09	2.07 ± 0.37
5	65.96 ± 0.66	21.97 ± 2.41	1.77 ± 0.27

4. *Attempted Identification and Isolation of the Final Products.* HPLC Analyses of reaction mixtures under acidic conditions (pH 3.7) show that in the absence of GA, quantitative conversion to the substituted phenol is achieved, this product being formed by the reaction of the aryl cation derived from 3MBD with H_2O, in keeping with previous HPLC reports [36][37]. However, upon increasing [GA], the ArOH concentration decreases (*Fig. 4*); but no new HPLC peaks were detected other than

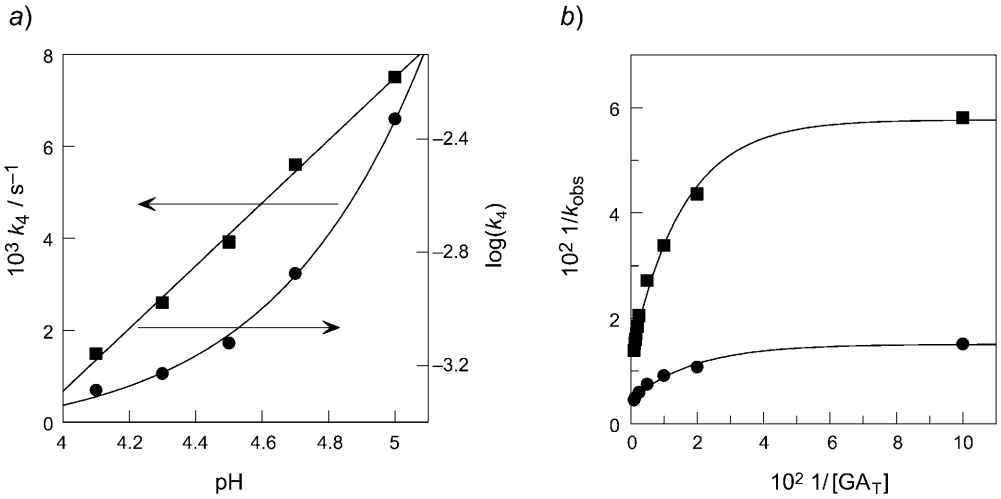

Fig. 3. a) *Variation of the intercept values in* Fig. 2, b (denoted as k_4, see text) *with pH and log plot showing a linear relationship between log*(k_4) *and pH.* b) *Representative double reciprocal plots of 1/*k_{obs} vs. *1/[*GA_T*] at two different pH.* ■ pH 4.5, ● pH 5.0. [GA_T] stands for the total or stoichiometric concentration of GA employed.

those associated with the solvent front; this suggests that, whatever product is formed, it must be very soluble and elutes with the front peak. Similar situations were found when analyzing the product distribution in reactions of toluenediazonium ions with ascorbic acid [17][23][24] and were attributed to the formation of the highly soluble, thermodynamically stable (*E*)-diazo ether.

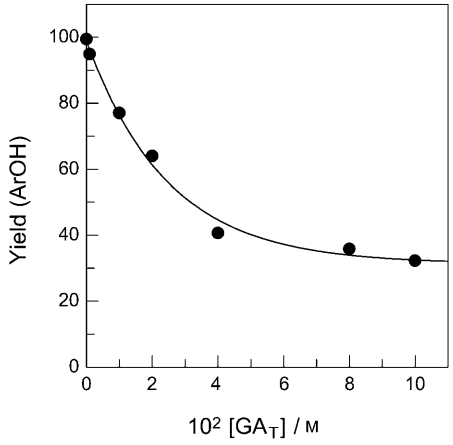

Fig. 4. *Variation in the yield of ArOH on increasing [GA] as determined by HPLC*

Inasmuch as total yields were less than 100%, careful purification and quantification of 3MBD was done, and large-scale reactions were carried out in attempts to provide substantial amounts of minor by-products for identification and quantification, but all efforts were unsuccessful. See *Exper. Part* for further details.

Discussion. – C-Coupling reactions are probably the EAS reactions characterized to the highest degree by its sensitivity to orientation. In practically all cases investigated, the aromatic substrate reacts only if strong electron donors are present, the reactivity order being $O^- > NR_2 > NHR > OR, OH \gg Me$. The reaction takes place exclusively at the *o*- and *p*-positions and, in fact, *m*-substitutions have never been observed [3][4][15]. The DFT results suggest that the second ionization of GA takes place in the 4-OH group (structure **1G** in *Scheme 2*), and given that the 1-, 3-, and 5-positions of GA are blocked by the carboxylate (C(1)) and the OH groups (C(3) and C(5)), they cannot be activated, and the reaction is not likely to proceed through a C-coupling mechanism.

The saturation-kinetics patterns found (*Fig. 2,b*) are also not compatible with the common EAS mechanism, and thus the results are suggestive of an O-coupling mechanism as was found for the reaction with methyl gallate. Moreover, the dependence of k_{obs} with the acidity (*Fig. 1*) indicates that the reaction is taking place through the dianionic form of GA, and the lack of a significant effect of base concentration on k_{obs} suggests that proton loss is not involved in the rate-limiting step and that the reaction is not general-base-catalyzed.

At relatively high acidities (*Fig. 2,a*), the variation of k_{obs} with [GA] is linear with intercept values very similar to that for the spontaneous decomposition of 3MBD [36]. However, at moderate acidities (*Fig. 2,b*), the k_{obs} *vs.* [GA] profiles follow saturation-kinetics patterns with unequal nonzero, pH-dependent intercepts (*Figs. 2,b* and *3,a*). While the saturation kinetics suggest the formation of an intermediate in a rapid pre-equilibrium step, the nonzero, pH-dependent intercepts cause the double reciprocal plots of $1/k_{obs}$ *vs.* 1/[GA] to curve as shown in *Fig. 3,b*. The finding of saturation kinetics where the intercept is different from zero contrasts with the experimental behavior found for the reaction with MG [19].

Given that the experimental results are not compatible with the predictions of a hypothetical C-coupling mechanism, and on the basis of the reaction mechanisms proposed for the reaction of ArN_2^+ ions with other antioxidants [19][20][22][23], we postulate the reaction mechanism shown in *Scheme 3* which involves the formation of a highly unstable (*Z*)-diazo ether which undergoes isomerization.

Scheme 3. *Proposed Reaction Mechanism between GA and 3MBD Comprising Two-Step Equilibrium Processes Leading to the Formation of Unstable (*Z*)- and (*E*)-Diazo Ethers*

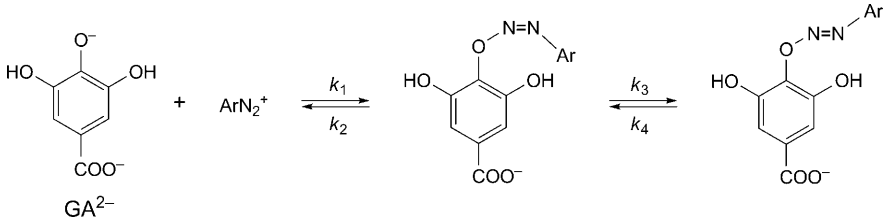

Eqn. 1 can be derived for a mechanism such as the following as shown by *Strickland et al.* [38] for enzyme-substrate or protein-ligand reactions, which take place through consecutive equilibrium processes involving the formation of a complex followed by an

isomerization or further reaction[1]). Note that in our case, B represents the reactive dianionic form of gallic acid.

$$A + B \underset{k_2}{\overset{k_1}{\rightleftharpoons}} C \underset{k_4}{\overset{k_3}{\rightleftharpoons}} D$$

$$k_{obs} = \frac{\dfrac{k_1 k_3 K_{a2}[GA_T]}{2[H^+]}}{\dfrac{k_1 K_{a2}[GA_T]}{2[H^+]} + k_2} + k_4 \quad (1)$$

Eqn. 1 predicts that when $[GA_T] \to 0$, $k_{obs} \to k_4$, consistent with the experimental observation of nonzero intercepts (*Fig. 2*). *Fig. 3,a* shows the dependence of k_4 on the acidity and that the plot of $\log(k_4)$ *vs.* pH is linear with a slope of 1.10 ± 0.04, suggesting an inverse dependence of k_4 with the acidity.

Alternatively, *Eqn. 1* can be rearranged to *Eqn. 2*, which predicts that a plot of $1/(k_{obs} - k_4)$ *vs.* $1/[GA_T]$ should be a straight line with an intercept value equal to k_3. *Fig. 5* shows that this prediction is fulfilled and from the slope and intercept values, the ratio k_1/k_2, which stands for the equilibrium constant of the first equilibrium step in *Scheme 2*, can be determined at the different working acidities (*Table 2*).

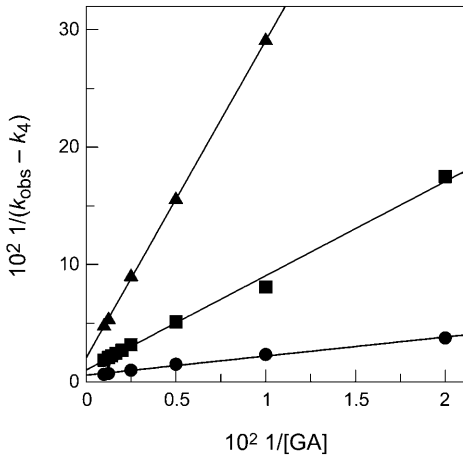

Fig. 5. *Double reciprocal plots according to* Eqn. 2 *at different acidities.* ▲ pH 4.1, ■ pH 4.5, ● pH 5.0. Data extracted from *Fig. 2*.

$$\frac{1}{k_{obs} - k_4} = \frac{2[H^+]k_2}{k_1 k_3 K_{a2}[GA_T]} + \frac{1}{k_3} \quad (2)$$

We attempted to estimate the values of k_1 and k_2 by introducing the determined k_3 and k_4 values in *Eqn. 1* and by fitting the (k_{obs}, $[GA_T]$) pairs of data using a nonlinear

[1]) Derivation of *Eqn. 1*, based on that previously reported by *Strickland et al.* [38], is provided as supplementary material, which may be obtained upon request from the authors.

least-squares method provided by the GraFit 5.0.5 computer program. The solid lines shown in *Fig. 2* are theoretical curves determined as just described; however, the k_1 and k_2 values obtained are statistically meaningless because the errors with which they are determined from the nonlinear fitting procedure are much higher than their own values, so they are not reported.

Further support for the proposed mechanism can be found by analyzing the variation of k_{obs} with $[GA_T]$ in those runs carried out at relatively high acidity (*Fig. 2,b*). Because $[H^+] >>> K_{a2}$, one may assume that $k_1K_{a2}[GA_T]/2[H^+] \ll k_2$, and thus *Eqn. 1* can be simplified to *Eqn. 3*, which predicts that a plot of k_{obs} *vs.* $1/[H^+]$ should be linear as illustrated in *Fig. 6*. The intercepts of these plots give values for k_4, which depend on the actual acid concentration employed, and at high acidities, k_4 should approach zero as shown in *Fig. 6*.

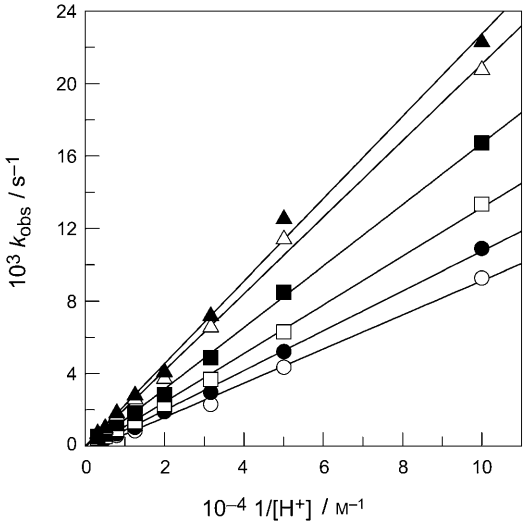

Fig. 6. *Linear variations of* k_{obs} *with the acidity according to* Eqn. 3 *at increasing [GA]*. ○ 0.05M ● 0.01M, □ 0.02M, ■ 0.04M, △ 0.08M, ▲ 0.1M. Data extracted from *Fig. 2*.

$$k_{obs} = \frac{k_1 k_3 K_{a2}}{2[H^+]k_2}[GA_T] + k_4 \qquad (3)$$

It is also worthwhile noting that at high acidity, the decomposition of 3MBD through the diazo ether route should be negligible because the concentration of the reactive dianionic species GA^{2-} present in the solution is very low, and thus the spontaneous decomposition of 3MBD (*Scheme 1,a*), becomes the main reaction taking place (*Fig. 2,a*).

As a final remark, it may be instructive to compare the proposed mechanism for the reaction of 3MBD with GA (*Scheme 3*) with that for the reaction of 3MBD with MG

which takes place through a saturation mechanism, and with that for a hypothetical single-step equilibrium mechanism. In the case of a reversible reaction of the type $A + B \rightleftharpoons C$, k_{obs} should be a linear function of [B] with a slope equal to the rate for the forward reaction and an intercept at zero [B] equal to that for the rate constant of the backward reaction [39]; this is certainly not the case as illustrated in *Fig. 2,b*. Alternatively, if k_4 in *Scheme 3* is negligibly small, the reaction scheme reflects a saturation-kinetics mechanism as was found in the reaction between 3MBD and MG [19]. In this case, *Eqn. 1* can be reduced to a hyperbolic form, and a plot of $1/k_{obs}$ *vs.* $1/[GA_T]$ should be linear, which is inconsistent with experimental data (*Fig. 3,b*). Thus, the proposed two-step mechanism seems the more credible.

Most of the studies on the stability of diazo ethers have been carried out in basic solutions as in the study of the reactions of ArN_2^+ ions with alkoxide or phenoxide compounds, which yield diazo ethers. Basically, the reaction of ArN_2^+ ions with methoxide ions occurs in three phases. The first is the very rapid formation of a (*Z*)-diazo methyl ether. In the second, some of the (*Z*)-diazo ether decomposes to yield reduction products (usually hydro-dediazoniation), and the rest is converted into the (*E*)-diazo ether.

Investigations by *Broxton* and *Roper* [40] confirmed that the initial reaction of the arenediazonium ions takes place in such a way that the (*Z*)-diazo ether is formed directly almost exclusively, and part of it is then transformed to the thermodynamically more stable (*E*)-isomer (which can in some instances be isolated) [20] by an ionization–recombination mechanism (*Broxton* and *Roper* [40]) or by a bond-rotating mechanism that has been described for *Sandmeyer* hydroxylations and chlorination reactions [41] but has not been extended to other systems.

In basic alcoholic solvents, reaction of ArN_2^+ ions with RO^- leads to the formation of unstable (*Z*)-diazo ethers which are rapidly converted into the more stable (*E*)-isomers. Previous studies [40][42][43] have shown that the rate of conversion of the (*Z*)- into the (*E*)-isomer is accelerated by electron-donating substituents at the aromatic ring, by decreasing the basicity of the alkoxide ion (MeO > EtO > i-PrO), and by solvents of greater ion-solvating power (MeOH > EtOH). In addition, it has been observed that decomposition of both (*Z*)- and (*E*)-isomers is very rapid on acidification of the solution, a feature that may hinder their study under a range of experimental conditions.

Conclusions. – The complex experimental behavior found for the reaction of 3MBD and GA indicates that the carboxylic group of GA has significant mechanistic consequences compared with the kinetic behavior found for the reaction between 3MBD and MG [19], even though the reaction with 3MBD takes place, in both cases, through the O-atom at the 4-position of the aromatic ring. The results demonstrate the complexity of the reactions between ArN_2^+ and polyhydroxylated phenolic antioxidants, mainly in those cases where the reaction takes place through the dianionic form of the antioxidant. These reactions have been very much less investigated than those with the mono- and dihydroxylated phenols [1][4], and deserve further work. Little is known about diazo ethers of the general structure ArN=NOR (with R = alkyl, aryl) except that they are rarely formed as stable products because they are very sensitive to acids, bases, and light [1][2][4][43]. It is also known that the ArN=NOR formed may

undergo subsequent isomerization or eventually may give rise to homolytic rupture of the bonds providing the initiation of a radical process [42–46].

Financial support from the following institutions is acknowledged: *Ministerio de Educación y Ciencia* (CTQ2006-13969-BQU), *Xunta de Galicia* (PGDIT06PXIB314249PR), *FEDER*, and Universidad de Vigo. We thank Prof. *H. Maskill* for helpful discussions, Prof. *María del Carmen Terán-Moldes* for her assistance with the experiments attempting the isolation of intermediates and the reaction products, and Prof. *Ricardo Mosquera-Castro* for his help with the computational chemistry. *S. L.-B.* thanks the *Ministerio de Educación y Ciencia* (*MEC*) for a *FPU* research training grant.

Experimental Part

Instrumentation. Electrochemical kinetic experiments were perfomed as indicated elsewhere [19] at constant temp. (T 30 ± 0.1°) by monitoring the decrease in the reduction peak of 3MBD at E_p *ca.* − 0.05 V. HPLC Data: *Waters*-HPLC system with a *W600* pump, a *W717* automatic injector, a *W2487* dual wavelength detector, and a computer for control and data storage; *Microsorb-MV-C-18* (*Rainin*) reversed-phase column (250 mm length, 3.9 mm internal diameter, and 4 μm particle size); mobile phase MeOH/H_2O 75:25 (*v*/*v*) containing 10^{-4} M HCl; injection volume 25 μl in all runs; UV detector at 210 nm.

UV/VIS Spectra and kinetic experiments: *Agilent-HP-8453*-UV/VIS spectrophotometer equipped with a thermostated cell carrier attached to a computer for data storage; kinetics were performed at constant temp. (T 30 ± 0.1°).

Materials. Reagents were of maximum purity available and used without further purification. Gallic acid and the reagents used for the preparation of 3-methylbenzenediazonium tetrafluoroborate, the acetic acid/acetate (AcOH/AcO^-), and the *Britton–Robinson* buffer were purchased from *Fluka* or *Aldrich* and used as received. Other materials used were from *Riedel de Haën*. All solns. were prepared by using *Milli-Q*-grade H_2O. Solns. employed in electrochemical measurements were bubbled with dry N_2 (99.999%) for at least 20 min and kept under N_2 during the measurements. The *Britton–Robinson* buffer was prepared by mixing H_3BO_3, AcOH, and H_3PO_4, and the pH was adjusted with conc. NaOH soln. Final concentrations of the electrolytes were 0.04M. The ionic strength I was adjusted to 0.2M by addition of KCl.

For 3MBD, see [19] (*cf.* [47][36]). The UV/VIS spectrum of a $1 \cdot 10^{-4}$ M aq. buffered (pH 1.6) GA soln. shows two absorption bands at λ 222 and 271 nm, resp. The wavelength of the absorption peak at λ 222 nm remained constant upon changing the pH of the soln. (pH 1.6–5) but the absorption band at λ 271 nm showed a hypsochromic shift of *ca.* 10 nm at pH 5.0, the exact position depending on the ionization state of GA. The first pK_a of GA is *ca.* 4.2 (associated to the ionization of the COOH group) at 25° [34][35], and subsequent alkalinization of the soln. leads to the ionization of the OH groups in the pyrogallol moiety, with $pK_{a2} = 8.55$ [34].

Methods. Reactions were followed electrochemically by monitoring 3MBD loss and diazo ether formation (*Fig. 7,a*), spectrometrically by monitoring the product formation at λ 416 nm (*Fig. 7,b*), or by employing a well-developed derivatization protocol [47][48] that exploits the rapid reaction between 3MBD and a suitable coupling agent to yield a stable azo dye (*Fig. 7,c*). In all electrochemical or spectrometric runs (monitoring the absorbance at λ 416 nm due to product formation), the experimental infinite value remained practically constant after leveling off, in contrast with the observed behavior in the reaction between 3MBD and MG, where a subsequent decrease in absorbance was detected [19].

Observed rate constants (k_{obs}) were obtained by fitting the absorbance–time or peak current-time data to the integrated first-order *Eqn. 4*, where M stands for the measured magnitude, obtained by a nonlinear least-squares method provided by a commercial computer program. Runs were done at T 30 ± 0.1° under pseudo-first-order conditions, and linear plots were obtained for more than $3t_{1/2}$. Duplicate or triplicate runs gave k_{obs} values within 5%.

$$\ln\left(\frac{M_1 - M_\infty}{M_0 - M_\infty}\right) = -k_{obs}t \qquad (4)$$

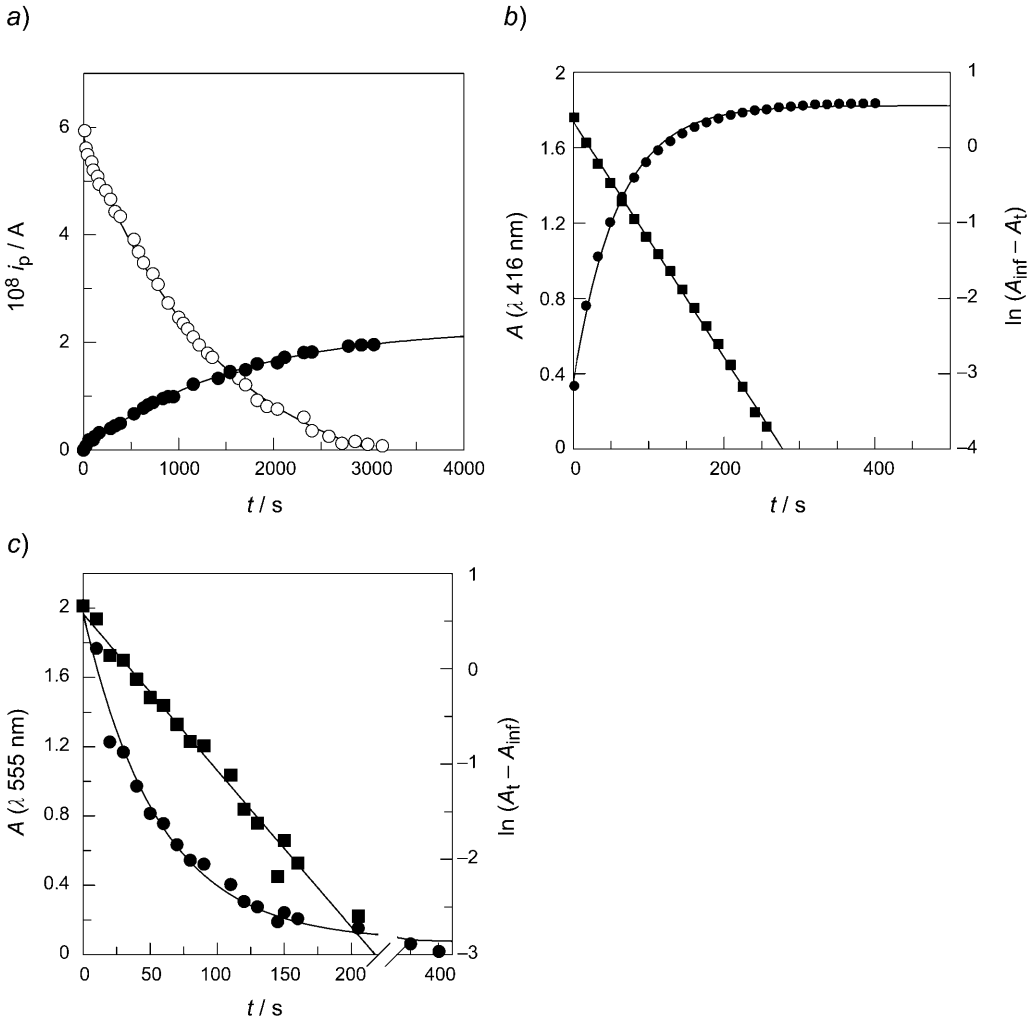

Fig. 7. *Illustrative kinetic plots:* a) *obtained by following the disappearance of 3MBD electrochemically as described elsewhere* [19], b) *by monitoring spectrometrically the formation of the products at λ 416 nm, and* c) *by monitoring spectrometrically the variation in the absorbance of the azo dye formed after derivatization of 3MBD as described elsewhere* [47][48]

Identification and Isolation of the Final Products. A number of attempts were made to isolate and identify the products of the reaction, but they were unsuccessful. In a typical experiment, 25 ml of an aq. acid soln. (pH 6.3, buffer control) containing GA (0.38 g, 0.0020 mol) was mixed with 25 ml of an aq. acid soln. containing 3MBD (0.5 g, 0.0024 mol) (→orange foam turning to reddish with time). The reaction was allowed to proceed to completion, and the products were extracted with 3×10 ml CH_2Cl_2 and subjected to column chromatography (activated (CH_2Cl_2/MeOH 97:3) silica gel). An intense yellow fraction eluted with solvent, and several different dark red fractions were collected. The yellow fraction was analyzed by TLC (hexane/AcOEt 97:3), and several spots were observed, indicative of the presence

of a variety of products making the attempts of isolation unsuccessful. Similar results were obtained when extraction was performed with solvents of different polarity.

On a semi-prep. scale, GA (0.19 g, 0.001 mol) was dissolved in 10 ml of a slightly acid aq. soln. (phosphate buffer control, pH 6) containing $KAl(SO_4)_2 \cdot 12\,H_2O$, and the mixture was placed in an ice bath with continuous stirring. Independently, 3MBD (0.25 g, 0.001 mol) was dissolved in 10 ml of an aq. acid soln. (pH 6). The reaction was initiated by adding dropwise the 3MBD soln. to the mixture containing GA (→ yellowish foam and reddish precipitate). The reaction was allowed to proceed to completion (*ca.* 15 min, ice bath). Then the precipitate was filtered under reduced pressure and subjected to recrystallization in hot EtOH; however, it turned darker immediately, and a tarry-like material was formed. Attempts to extract the products with common org. solvents such as CH_2Cl_2, hexane, or AcOEt led to the formation of intractable tarry materials, indicating that the nature of the solvent is crucial to the stability of the formed products.

The results obtained were not totally surprising because we already reported in previous work [19] unsuccessful attempts to identify and isolate the products formed in the course of the reaction between 3MBD and methyl gallate, highlighting the high instability of the products of the reaction.

REFERENCES

[1] A. F. Hegarty, 'Kinetics and Mechanisms of Reactions Involving Diazonium and Diazo Groups', in 'The Chemistry of Diazonium and Diazo Compounds', Part 1, Ed. S. Patai, J. Wiley & Sons, New York, 1978.
[2] K. H. Saunders, R. L. M. Allen, 'Aromatic Diazo Compounds', 3rd edn., Edward Arnold, Baltimore, MD, 1985.
[3] H. Zollinger, 'Color Chemistry', VCH, Weinheim, Germany, 1991.
[4] H. Zollinger, 'Diazo Chemistry I, Aromatic and Heteroaromatic Compounds', VCH, Weinheim, Germany, 1994.
[5] B. M. Tracey, D. E. G. Shuker, *Chem. Res. Toxicol.* **1997**, *10*, 1378.
[6] L. Copolovici, I. Baldea, *Anal. Bioanal. Chem.* **2002**, *374*, 13.
[7] J. S. Esteve-Romero, E. F. Simó-Alfonso, M. C. García-Alvarez-Coque, G. Ramis-Ramos, *Trends Anal. Chem.* **1995** *14*, 29.
[8] M. C. García-Alvarez-Coque, E. F. Simó-Alfonso, G. Ramis-Ramos, J. S. Esteve-Romero, *J. Pharm. Biomed. Anal.* **1995**, *13*, 237.
[9] S. Yamato, K. Kobayashi, K. Ebara, K. Shimada, S. Ohta, *Biol. Pharm. Bull.* **2003**, *26*, 397.
[10] T. M. Bockman, D. Kosynkin, J. K. Kochi, *J. Org. Chem.* **1997**, *62*, 5811.
[11] S. V. Rosokha, J. K. Kochi, *J. Org. Chem.* **2002**, *67*, 1727.
[12] C. Boga, J. Degani, E. Del Vecchio, R. Fochi, L. Forlani, P. Todesco, *Eur. J. Org. Chem.* **2002**, *2002*, 3837.
[13] C. Boga, E. Del Vecchio, L. Forlani, *Eur. J. Org. Chem.* **2004**, *7*, 1567.
[14] C. Boga, E. Del Vecchio, L. Forlani, A. Mazzanti, P. E. Todesco, *Angew. Chem., Int. Ed.* **2005**, *44*, 3285.
[15] I. Szele, H. Zollinger, 'Azo Coupling Reactions: Structure and Mechanism', in 'Preparative Organic Chemistry', Springer-Verlag, New York, 1986.
[16] O. Machackova, V. Sterba, K. Valter, *Collect. Czech. Chem. Commun.* **1972**, *37*, 1851.
[17] U. Costas-Costas, E. González-Romero, C. Bravo-Díaz, *Helv. Chim. Acta* **2001**, *84*, 632.
[18] U. Costas-Costas, C. Bravo-Díaz, E. González-Romero, *Langmuir* **2004**, *20*, 1631.
[19] S. Losada-Barreiro, V. Sánchez-Paz, C. Bravo-Díaz, *Helv. Chim. Acta* **2007**, *90*, 1559.
[20] M. P. Doyle, C. L. Nesloney, M. S. Shanklin, C. A. Marsh, K. C. Brown, *J. Org. Chem.* **1989**, *54*, 3785.
[21] E. González-Romero, B. Malvido-Hermelo, C. Bravo-Díaz, *Langmuir* **2002**, *18*, 46.
[22] S. Losada-Barreiro, V. Sánchez-Paz, M. J. Pastoriza-Gallego, C. Bravo-Díaz, *Helv. Chim. Acta* **2008**, *90*, 21.
[23] U. Costas-Costas, C. Bravo-Díaz, E. González-Romero, *Langmuir* **2005**, *21*, 10983.
[24] U. Costas-Costas, C. Bravo-Díaz, E. González-Romero, *Langmuir* **2003**, *19*, 5197.

[25] K. Gunaseelan, L. S. Romsted, E. González-Romero, C. Bravo-Díaz, *Langmuir* **2004**, *20*, 3047.
[26] K. Gunaseelan, L. S. Romsted, M. J. Pastoriza-Gallego, E. González-Romero, C. Bravo-Díaz, *Adv. Colloid Interface Sci.* **2006**, *123–126*, 303.
[27] O. I. Aruoma, A. Murcia, J. Butler, B. Halliwell, *J. Agric. Food. Chem.* **1993**, *41*, 1880.
[28] O. I. Aruoma, 'Free Radicals and Antioxidants in Food Science', Chapman & Hall, London, UK, 1998.
[29] C. Capelli, B. Mennuci, S. Monti, *J. Phys. Chem. A* **2005**, *109*, 1933.
[30] E. N. Frankel, A. S. Meyer, *J. Sci. Food Agric.* **2000**, *80*, 1925.
[31] D. J. McClemments, E. A. Decker, *J. Food Sci.* **2000**, *65*, 1270.
[32] V. Tulyathan, R. Boulton, V. Singleton, *J. Agric. Food Chem.* **1989**, *37*, 844.
[33] N. Takenaka, M. Tanaka, K. Okitsu, H. Bandow, *J. Phys. Chem. A* **2006**, *110*, 10628.
[34] N. Binbuga, K. Chambers, W. P. Henry, T. P. Schultz, *Holzforschung* **2005**, *59*, 205.
[35] CRC, ' Handbook of Chemistry and Physics', 78th edn., CRC Press, Boca Raton, 1997.
[36] R. Pazo-Llorente, M. J. Rodriguez-Sarabia, E. González-Romero, C. Bravo-Díaz, *Int. J. Chem. Kinet.* **1999**, *31*, 73.
[37] R. Pazo-Llorente, C. Bravo-Díaz, E. González-Romero, *Eur. J. Org. Chem.* **2003**, *2003*, 3421.
[38] S. Strickland, G. Palmer, V. Massey, *J. Biol. Chem.* **1975**, *250*, 4048.
[39] J. H. Espenson, 'Chemical Kinetics and Reaction Mechanisms', 2nd edn., McGraw-Hill, New York, 1995.
[40] T. J. Broxton, D. L. Roper, *J. Org. Chem.* **1976**, *41*, 2157.
[41] P. Hanson, J. R. Jones, A. B. Taylor, P. H. Walton, A. W. Timms, *J. Chem. Soc., Perkin Trans. 2* **2002**, 1135.
[42] W. J. Boyle, T. Broxton, J. F. Bunnett, *J. Chem. Soc., Chem. Commun.* **1971**, 1470.
[43] T. J. Broxton, A. C. Stray, *J. Org. Chem.* **1980**, *45*, 2409.
[44] T. J. Broxton, M. J. McLeish, *J. Org. Chem.* **1982**, *47*, 3673.
[45] R. Pazo-Llorente, C. Bravo-Díaz, E. González-Romero, *Eur. J. Org. Chem.* **2004**, *2004*, 3221.
[46] R. Pazo-Llorente, H. Maskill, C. Bravo-Díaz, E. González-Romero, *Eur. J. Org. Chem.* **2006**, *2006*, 2201.
[47] M. C. García-Meijide, C. Bravo-Díaz, L. S. Romsted, *Int. J. Chem. Kinet.* **1998**, *30*, 31.
[48] C. Bravo-Díaz, E. González-Romero, *J. Chromatogr., A* **2003**, *989*, 221.

Received March 9, 2009